Materials Science & Engineering A 853 (2022) 143778

Contents lists available at ScienceDirect

Materials Science & Engineering A

journal homepage: www.elsevier.com/locate/msea

Achieving high tensile ductility in a fully nanostructured Al–Mg alloy by low-temperature annealing

S.B. Zhao [a], Y. Yan [a], X.W. Li [a], P. Xue [b,**], D.R. Ni [b], Z.Y. Ma [b], Y.Z. Tian [c,*]

[a] Department of Materials Physics and Chemistry, School of Materials Science and Engineering, Northeastern University, Shenyang, 110819, China
[b] Shi-changxu Innovation Center for Advanced Materials, Institute of Metal Research, Chinese Academy of Sciences, Shenyang, 110016, China
[c] Key Laboratory for Anisotropy and Texture of Materials (Ministry of Education), School of Materials Science and Engineering, Northeastern University, Shenyang, 110819, China

ARTICLE INFO

Keywords:
Al-Mg alloy
Cold rolling
Annealing
Nanostructure
Ductility

ABSTRACT

Low ductility has always been a drawback for nanostructured materials. In this study, we applied a low-temperature annealing process on a cold rolled Al-8.1Mg-0.15Zr alloy with supersaturated state. It is found that the uniform elongation of the rolled specimen was improved by 124% after a low-temperature annealing treatment at 333 K, while an enhanced tensile strength was obtained in the annealed specimen. The good combination of tensile strength and ductility was mainly attributed to the fully nanostructured microstructure and the formation of nanoscale precipitates and segregation of Mg element after annealing treatment.

1. Introduction

In recent years, on account of the increasingly severe resource and environment problems, massive efforts have been paid to advocate the strong demand of energy conservation and emission reduction [1]. Al–Mg alloys (5xxx series Al alloy) that mainly contain Mg element have been widely used in marine, aerospace and automotive fields due to their low density, excellent corrosion resistance, high specific strength, good workability and weldability [2–5]. It has been reported that the yield strength (YS) of the alloy increases significantly from 290 MPa to 510 MPa with the magnitude of Mg content from 1% to 7% by equal-channel angular pressing (ECAP) [6]. Solid solution strengthening and work hardening are generally responsible for enhancing the mechanical properties of Al–Mg alloys [7–9]. Apart from the Mg atoms, it is found that the mechanical performance of Al–Mg alloys can be further enhanced by appropriate addition of Zr element [10]. Al_3Zr particles are generated due to the reaction between these Zr atoms and Al matrix, by which dislocations can be pinned to improve strengthening effect of Al–Mg alloys [11,12].

Generally, the Mg content of Al–Mg alloys is no more than 6% due to the formation of continuous or discontinuous β phase along grain boundaries (GBs), which leads to intergranular corrosion and stress corrosion cracking [13]. However, there is still vast composition space for utilizing the solid solution strengthening effect via Mg addition. Recent studies indicated that the strength can be further enhanced by increasing Mg content of 9% [14]. In this case, it is feasible to ameliorate the mechanical properties by changing the Mg content. Besides the chemical composition, plastic deformation strategies in the form of cold rolling or ECAP have been frequently employed to enhance the strength. However, these nanostructured Al–Mg alloys usually possess high strength but low ductility due to the excessive dislocations [6,15], which is detrimental to their industrial applications. The ductility can be retained in the subsequent annealing, however, the strength is deteriorated dramatically due to apparent grain growth [16]. In order to retain high strength and promising uniform ductility collectively, proper heat treatments should be carefully designed and applied.

In this work, multiple strategies of high Mg content, intense rolling strain and low temperature annealing were employed together to ameliorate the mechanical properties including tensile strength and uniform elongation in an Al–Mg–Zr alloy.

2. Experimental method

The Al-8.1Mg-0.15Zr (wt.%) alloy was cast by the vacuum induction method, then the plate with nanostructured microstructure was prepared by rolling and annealing, and the processing route is illustrated in

* Corresponding author.
** Corresponding author.
E-mail addresses: pxue@imr.ac.cn (P. Xue), tianyanzhong@mail.neu.edu.cn (Y.Z. Tian).

https://doi.org/10.1016/j.msea.2022.143778
Received 8 March 2022; Received in revised form 3 August 2022; Accepted 6 August 2022
Available online 12 August 2022
0921-5093/

Fig. 1. To achieve the complete solution of Mg in Al matrix, Al-8.1Mg-0.15Zr alloy was solution treated at the temperature of 753 K for 12 h and then quenched in water (solution). Following that, the alloy was rolled from 11 mm to 1 mm at room temperature, which corresponds to a reduction in thickness of 91% (as-rolled). To avoid the temperature rise during the rolling process, the sheet was immediately immerged into water after each rolling pass. After intense cold rolling deformation, the samples were heat treated at a low temperature of 333 K for 48 h (annealed).

The microstructures of Al-8.1Mg-0.15Zr alloy were examined by optical microscopy (OM), electron backscatter diffraction (EBSD) and transmission electron microscopy (TEM, Tecnai F20) equipped with energy dispersive spectroscopy (EDS). The EBSD system is equipped on a field emission scanning electron microscope (FE-SEM, FEI Inspect F50). An accelerating voltage of 20 kV, a working distance of 10 mm and a step size of 100 nm were used to acquire the EBSD map. The TSL OIM Analysis 7 software was used to analyze the ESBD data. TEM characterization was conducted on an FEI Tecnai F20 with an accelerating voltage of 200 kV. EBSD specimens were prepared by electropolishing at 12 V for 90 s at 248 K using an electrolyte consisting of 90 vol% ethanol and 10 vol% perchloric acid. Thin foils for TEM characterization were prepared by twin-jet electropolishing at 12 V using an electrolyte consisting of 70 vol% methanol and 30 vol% nitric acid at 248 K. The RD-ND (RD: rolling direction; ND: normal direction) plane of the as-rolled and annealed specimen was characterized. To identify the precipitates during annealing treatment and to quantify the dislocation density, X-ray diffraction (XRD, SmartLab) was performed with a scanning speed of 10°/min from 35° to 80°. Tensile tests were conducted at an initial strain rate of 10^{-3} s^{-1} by using a universal tensile testing machine (Instron 8801), and the samples were cut parallel to the rolling direction with a gauge size of 10 × 4 × 1 mm.

3. Results and discussions

Fig. 2 shows the microstructure and element distribution of the solution-treated alloy. It is obvious from the optical micrograph that the solution-treated samples exhibited relatively uniform equiaxed grains with the mean grain size of about 150 μm (Fig. 2(a)). The microstructures were further characterized by TEM, as shown in Fig. 2(b). Combined with the EDS mapping corresponding to Al, Mg and Zr elements, it is concluded that the particles were enriched with Zr atoms. In addition, it can be seen that the distribution of Mg element was quite homogeneous, indicating that Mg atoms were fully dissolved in the matrix after solid solution treatment.

EBSD characterizations were performed on the as-rolled and annealed alloys, respectively, as shown in Fig. 3. Different from the solution-treated alloys, the grains of as-rolled alloys are elongated along the rolling direction, presenting the banded pattern due to severe rolling deformation (Fig. 3(a)). Apparently, the grains pattern after the annealing treatment (Fig. 3(d)), irrespective of grain sizes, was similar to that of the as-rolled specimen. It should be noted that the indexed degree of the grains is low by EBSD, leaving many dark areas regarded as high-density dislocations and nanograins [7]. These results indicate that low temperature annealing in this work did not induce recrystallization.

It is further proved by the TEM images in Fig. 3(b,e). The average bandwidth of the as-rolled and annealed specimens were estimated as 78 ± 17 nm and 86 ± 19 nm, respectively (Fig. 3(c) and (f)). Considering the short annealing time and the low annealing temperature, the change in grain size is not significant although the dislocation entanglement had recovered to some extent after annealing. It is now clear that low temperature annealing at 333 K in this work did not induce recrystallization and had retained the fully nanostructured grains, which is critical for achieving high strength.

The detailed microstructure of the annealed sample was further characterized by scanning TEM (STEM), as shown in Fig. 4. In contrast to the homogeneous elemental distribution, Mg and Zr segregation was activated after low-temperature annealing and precipitates can be observed from the EDS mapping. To determine the phase changes during the annealing process, XRD analysis was performed on the three kinds of specimens, as shown in Fig. 5. Different from the XRD results of the solid-solution and as-rolled alloys that exhibit simple single-phase structure, apparent Al_3Zr and Al_3Mg_2 phases are detected after the annealing treatment. The lattice parameter of Al–Mg alloys decreases with reducing Mg content in the solid solution due to the precipitations and the clusters of solute atoms [14]. Based on the lattice parameters given by XRD, the mass fractions of Mg in the as-rolled and annealed states are decreased by 0.19% and 1.09%, respectively, in contrast to the solid solution state. Combined with the XRD and EDS mapping results, it can be concluded that the formation of Al_3Mg_2 nanoparticles is induced by the segregation of Mg atoms during the low-temperature annealing process. These newly formed precipitates and retained nanostructure after annealing might impact on the mechanical properties, which will be examined in the following section.

The engineering stress-strain curves of the Al-8.1Mg-0.15Zr alloys under as-rolled and annealed states are shown in Fig. 6(a). Comparable YS of 449 ± 16 MPa and 440 ± 15 MPa were obtained in the as-rolled and annealed specimens, respectively, obviously higher than that of traditional Al–Mg alloys with less Mg element addition [14,17]. Moreover, the ultimate tensile strength (UTS) of the annealed specimen increased to 544 ± 8 MPa, which was higher than that of the as-rolled specimen (525 ± 5 MPa). The enhanced strength in the annealed specimen can be attributed to the retained nanostructure and prolonged strain-hardening capability.

Remarkably, due to the formation of Al_3Zr dispersoids, the uniform elongation of the annealed specimen (~10.3 ± 0.2%) was increased by 124% compared to that of as-rolled specimen (~4.6 ± 0.3%), which is striking for fully nanocrystalline materials [18]. Meanwhile, the tensile curve of the annealed specimen showed a slight serration behavior. However, the serration behavior has been frequently observed in coarse-grained Al–Mg alloys, which is supposed to be induced by Portevin–Le Chatelier (PLC) effect [19]. The reduction of serration behavior in this work can be attributed to the trapping effect of Al_3Zr and Al_3Mg_2 nanoparticles in the nanostructured matrix, resulting in a lower diffusivity of Mg solute atoms. Thus, the time interval between dislocation pinning and unpinning is reduced, relieving the PLC effect in the alloy [18]. It can be seen from Fig. 6(b) that the strain-hardening rate (θ) of the annealed specimens was higher than that of as-rolled specimen, which delayed the necking process and significantly enhanced the uniform elongation. Therefore, it can be concluded that low-temperature annealing can exert a significant impact on the

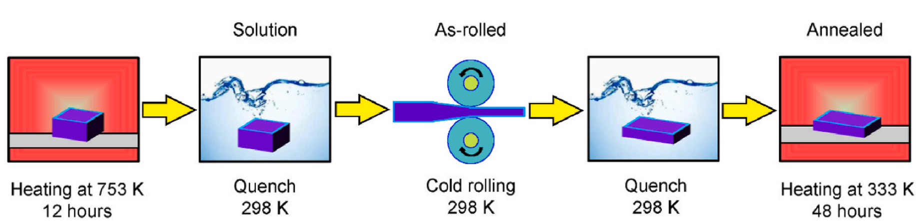

Fig. 1. Processing route of the Al–Mg alloy.

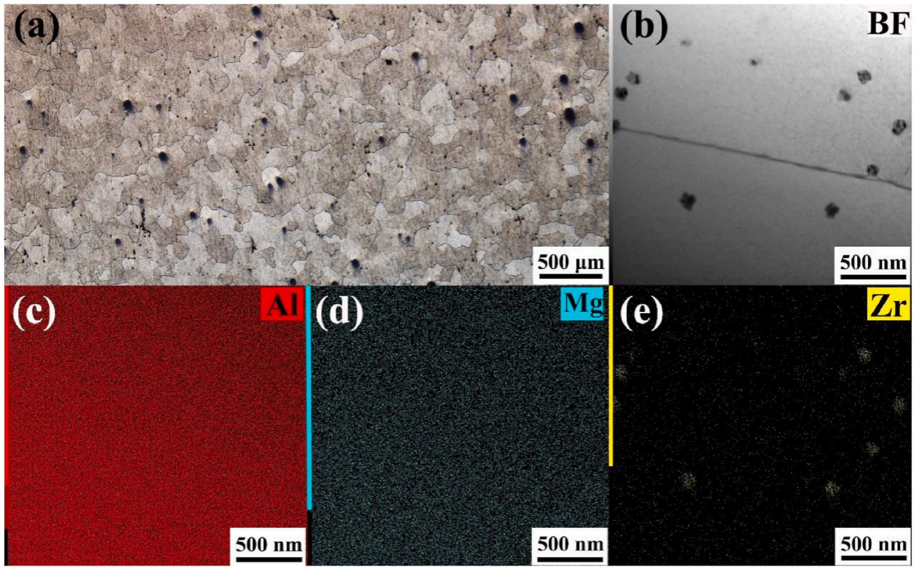

Fig. 2. (a) OM and (b) TEM images of the solid-soluted Al–Mg alloy; (c–e) elemental mapping of Al, Mg and Zr elements in (b).

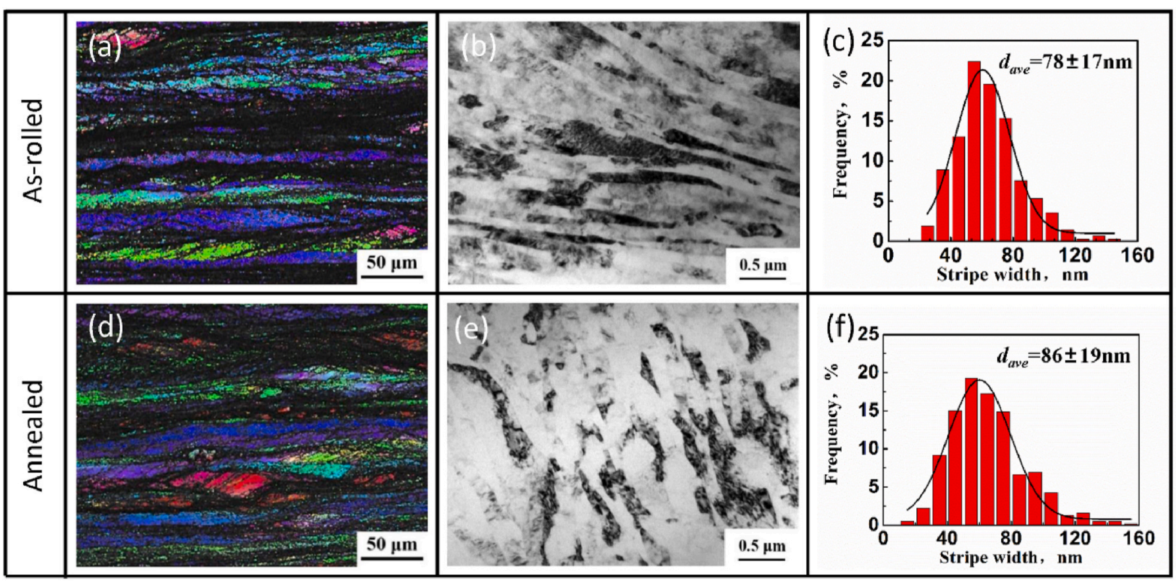

Fig. 3. EBSD images of (a) as-rolled and (d) annealed sample; TEM images and statistical results of bandwidth of (b,c) as-rolled and (e,f) annealed sample.

mechanical properties of the as-rolled Al–Mg alloy.

It is apparent from Fig. 6 that low-temperature annealing improves the ductility without losing YS too much and even raises the UTS, which is quite striking for the fully nanostructured specimen. The attainment of improved strain-hardening capability after annealing can be attributed to different origins. First, the dislocations interaction with precipitates is promoted. In contrast to the as-rolled specimen that has a simple single-phase solid solution, nanoscale Al_3Mg_2 and Al_3Zr precipitates appear after low-temperature annealing, which are supposed to pin dislocations efficiently during tensile tests. These Al_3Zr precipitates are reported to have a $L1_2$ structure and impact strong strengthening effect via the Orowan mechanism [18,20]. Ninomiya et al. [21] added 0.2 wt%Zr to high-purity Al-8wt.%Mg alloy, and found that the addition of Zr suppressed intergranular fracture at 298 K after solution treatment. As a result, the elongation to failure was improved by 21% by the addition of Zr. Second, the recovered microstructure can provide ample room for dislocations storage. Cross slip was inhibited in Al–Mg alloys with high Mg content as the stacking fault energy decreases with increasing Mg content [7]. As a result, supersaturated dislocations were stored in the as-rolled specimen. In the subsequent annealing process, these excessive dislocations can recover and the dislocation density decreases, as shown in Table 1.

The mean dislocation density can be calculated generally by the following equation [22]:

$$\rho = 2\sqrt{3}\left(\varepsilon^2\right)^{\frac{1}{2}} \Big/ (D \times b) \tag{1}$$

where ρ is the mean dislocation density, ε is the average micro strain, D is the average band size, and b is the Burgers vector. The value of ε was given by further analyzing the XRD results. These corresponding values are listed in Table 1. It can be seen that the values of ε and ρ for annealed samples are smaller than those of as-rolled samples, further confirming the occurrence of recovery during the annealing treatment. Therefore, the annealed specimen can retain the capability to store dislocations during tensile tests.

The YS of these two specimens was also evaluated according to the

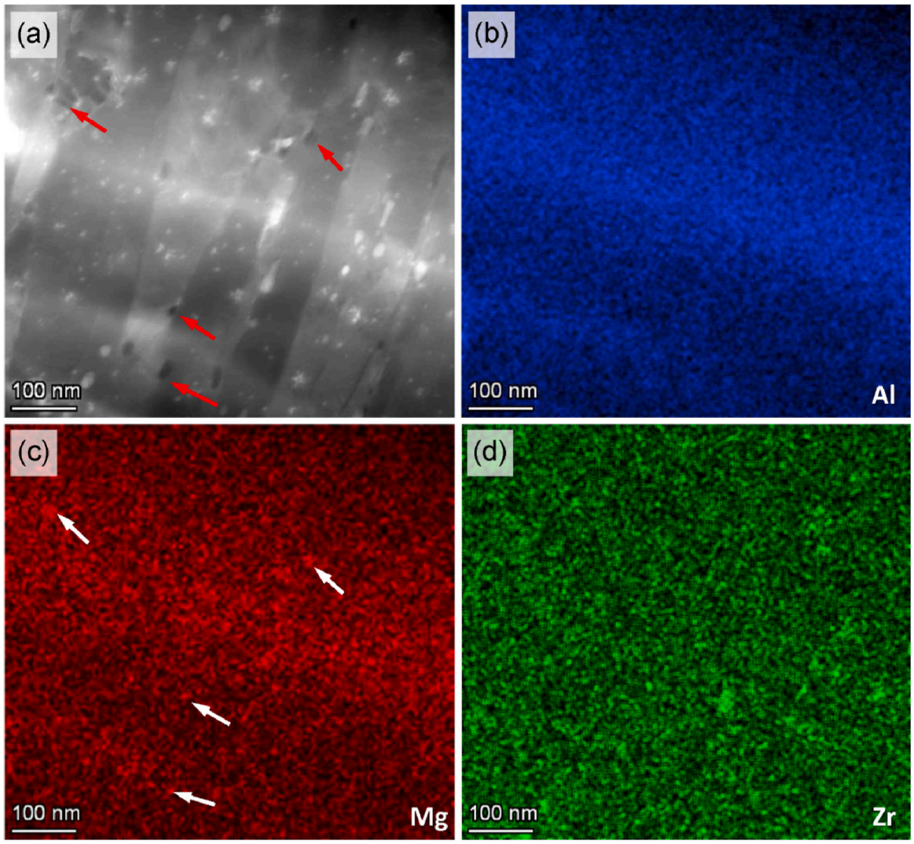

Fig. 4. (a) Scanning TEM image and (b–d) EDS mapping results of the annealed Al-8.1Mg-0.15Zr alloy. The arrows in (a,c) indicated the Mg-rich phase.

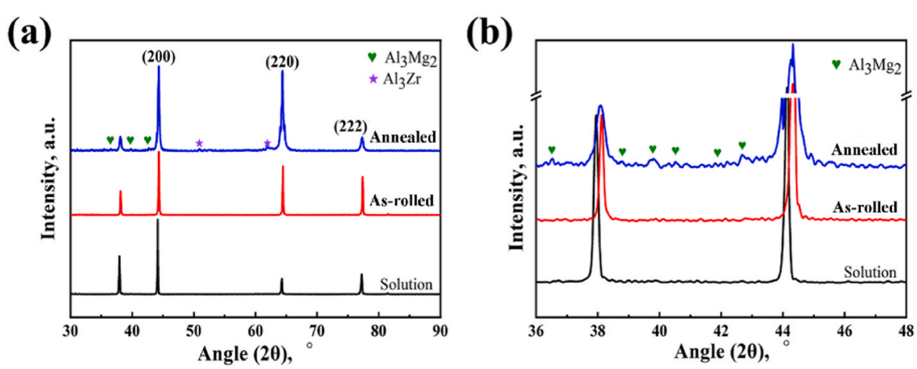

Fig. 5. (a) XRD patterns and (b) the magnified diffraction peak from 36° to 46° for solid solution, as-rolled and annealed samples.

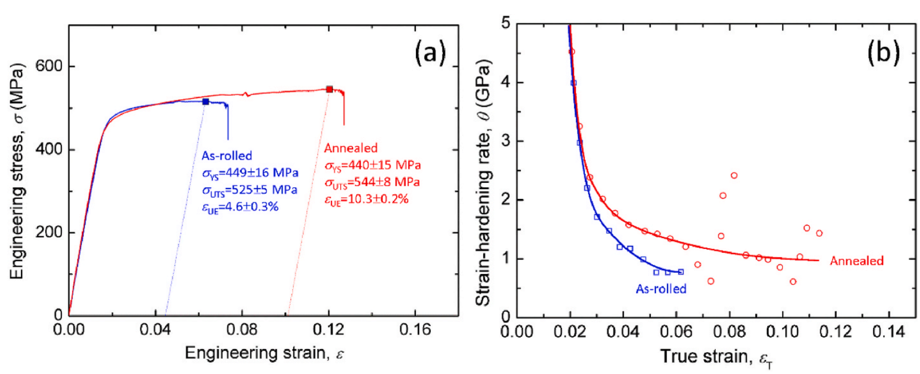

Fig. 6. (a) Engineering stress-strain curves and (b) strain-hardening curves of the as-rolled and annealed samples.

Table 1
Values of ε and ρ of samples with different processing conditions.

Condition	Lattice micro strain ε	Dislocation density ρ/m^{-2}
As-rolled	2.46×10^{-3}	3.820×10^{14}
Annealed	1.79×10^{-3}	2.521×10^{14}

following equations:

$$\sigma_y = \Delta\sigma_{SS} + \Delta\sigma_D + \Delta\sigma_{band} \quad (2)$$

$$\Delta\sigma_{SS} = \sigma_0 + HC^n \quad (3)$$

$$\Delta\sigma_D = \alpha MGb\sqrt{\rho} \quad (4)$$

$$\Delta\sigma_{band} = k_{band}D^{-\frac{1}{2}} \quad (5)$$

where $\Delta\sigma_{SS}$ is the solid solution strengthening, σ_0 is the lattice friction stress, which is very low in face-centered cubic metals (such as Al) [23], $\Delta\sigma_D$ is the dislocation strengthening, $\Delta\sigma_{band}$ is the band structure strengthening; The constants $H = 13.8$ MPa/wt.%, $n = 1.04$ and C is the solute concentration (in wt.%) [24], and the corresponding values for as-rolled and annealed states are 7.81 and 6.91, respectively, by converting lattice parameters; α is a constant (0.3 [25]), M is the Taylor factor (3.06 [26]), G is the shear modulus (27 GPa [6]), and k_{band} value is 1/4 of k_y (0.22 MPa m$^{1/2}$ [27]).

According to the above equations, the σ_y value of the as-rolled specimen was calculated to be 452.4 MPa, which basically matches well with the experimental results; in contrast, the σ_y of the annealed specimen was calculated as 403.1 MPa, which is lower than the experimental data. Two possible mechanisms are responsible for the discrepancy. First, apparent Al_3Mg_2 and Al_3Zr nanoparticles are detected after annealing, however, their roles cannot be estimated qualitatively due to the limited amount and heterogeneous distribution. Second, recovery of a nanostructure can induce abnormal hardening [28]. Huang et al. [28] reported the annealing-induced hardening and deformation-induced softening phenomenon in a nanostructured pure Al, which is just opposite to the well accepted conclusions based on classical physical metallurgy. When a deformed structure is annealed at a low temperature that does not cause recrystallization, typical effects include a coarsening of boundary spacing, recovery of low-angle boundaries, and reduction in the dislocation density in the grain interior, at grain boundaries and triple junctions [28]. These microstructure changes apply to the present work, and are supposed to reduce the dislocation sources, which make it difficult to activate new dislocation source and raise σ_y of nanostructured materials.

4. Conclusions

In this work, nanostructured Al-8.1Mg-0.2Zr alloy with high YS of 449 ± 16 MPa and UTS of 525 ± 5 MPa was processed by severe cold rolling deformation. Following the low-temperature annealing at 333 K for 48 h, comparable YS of 440 ± 15 MPa with an enhanced UTS of 544 ± 8 MPa were obtained due to the retained fully nanostructured microstructure. Meanwhile, the uniform elongation of the rolled specimen (4.6 ± 0.3%) was improved by 124% after low-temperature annealing treatment (10.3 ± 0.2%), which is induced by manipulating Mg and Zr element segregation and forming nanoparticles. This work provides an effective method to improve the tensile ductility of nanostructured materials.

CRediT authorship contribution statement

S.B. Zhao: Data curation, Writing – original draft. **Y. Yan:** Supervision, Writing – review & editing. **X.W. Li:** Writing – review & editing. **P. Xue:** Resources, Writing – review & editing. **D.R. Ni:** Investigation, Writing – review & editing. **Z.Y. Ma:** Resources, Writing – review & editing. **Y.Z. Tian:** Conceptualization, Writing – review & editing.

Declaration of competing interest

The authors declare that they have no known competing financial interests or personal relationships that could have appeared to influence the work reported in this paper.

Data availability

Data will be made available on request.

Acknowledgements

This work was supported by the National Natural Science Foundation of China under Grant No. 52071317, the Fundamental Research Funds for the Central Universities (No. N2102008), Liaoning Province Excellent Youth Foundation (2021-YQ-01), and the Youth Innovation Promotion Association of the Chinese Academy of Sciences (Y2021061).

References

[1] S. Lathabai, P. G Lloyd, The effect of scandium on the microstructure, mechanical properties and weldability of a cast Al–Mg alloy, Acta Mater. 50 (2002) 4275–4292.
[2] W.S. Miller, L. Zhuang, J. Bottema, A.J. Wittebrood, P. De Smet, A. Haszler, A. Vieregge, Recent development in aluminium alloys for the automotive industry, Mater. Sci. Eng., A 280 (2000) 37–49.
[3] A. Filatov Yu, V.I. Yelagin, V.V. Zakharrov, New Al–Mg–Sc alloys, Mater. Sci. Eng., A 280 (2000) 97–101.
[4] A.K. Godasu, A. Kumar, S. Mula, Influence of cryocooling on friction stir processing of Al-5083 alloy, Mater. Manuf. Process. 35 (2020) 202–213.
[5] Y. Liu, M. Liu, X. Chen, Y. Cao, H.J. Roven, M. Murashkin, R.Z. Valiev, H. Zhou, Effect of Mg on microstructure and mechanical properties of Al-Mg alloys produced by high pressure torsion, Scripta Mater. 159 (2019) 137–141.
[6] M. Zha, Y. Li, R.H. Mathiesen, R. Bjørge, H.J. Roven, Microstructure evolution and mechanical behavior of a binary Al-7Mg alloy processed by equal-channel angular pressing, Acta Mater. 84 (2015) 42–54.
[7] D. Jang, Y. Park, W. Kim, Significant strengthening in superlight Al-Mg alloy with an exceptionally large amount of Mg (13 wt%) after cold rolling, Mater. Sci. Eng., A 744 (2019) 36–44.
[8] B.H. Lee, S.H. Kim, J.H. Park, H.W. Kim, J.C. Lee, Role of Mg in simultaneously improving the strength and ductility of Al–Mg alloys, Mater. Sci. Eng., A 657 (2016) 115–122.
[9] V. Ocenasek, M. Slamova, Resistance to recrystallization due to Sc and Zr addition to Al-Mg alloys, Mater. Char. 47 (2001) 157–162.
[10] Y.J. Chen, Y.C. Chai, H.J. Roven, S.S. Gireesh, Y.D. Yu, J. Hjelen, Microstructure and mechanical properties of Al–xMg alloys processed by room temperature ECAP, Mater. Sci. Eng., A 545 (2012) 139–147.
[11] P.J. Apps, M. Berta, P.B. Prangnell, The effect of dispersoids on the grain refinement mechanisms during deformation of aluminum alloys to ultra-high strains, Acta Mater. 53 (2005) 499–511.
[12] C.Y. Barlow, N. Hansen, Y.L. Liu, Fine scale structures from deformation of aluminum containing small alumina particles, Acta Mater. 50 (2002) 171–182.
[13] R.H. Jones, D.R. Baer, M.J. Danielson, J.S. Vetrano, Role of Mg in the stress corrosion cracking of an Al-Mg alloy, Metall. Mater. Trans. A 32 (2001) 1699–1711.
[14] M. Zha, X.T. Meng, H.M. Zhang, X.H. Zhang, H.L. Jia, Y.J. Li, J.Y. Zhang, H. Y. Wang, Q.C. Jiang, High strength and ductile high solid solution Al–Mg alloy processed by a novel hard-plate rolling route, J. Alloys Compd. 728 (2017) 872–877.
[15] M. Zha, H.M. Zhang, Z.Y. Yu, X.H. Zhang, X.T. Meng, H.Y. Wang, Q.C. Jiang, Bimodal microstructure - a feasible strategy for high-strength and ductile metallic materials, J. Mater. Sci. Technol. 34 (2018) 257–264.
[16] V. Kulitskiy, S. Malopheyev, S. Mironov, R. Kaibyshev, Grain refinement in an Al-Mg-Sc alloy: equal channel angular pressing versus friction-stir processing, Mater. Sci. Eng., A 674 (2016) 480–490.
[17] M. Zha, Y. Li, R.H. Mathiesen, R. Bjørge, H.J. Roven, Achieve high ductility and strength in an Al-Mg alloy by severe plastic deformation combined with inter-pass annealing, Mater. Sci. Eng., A 598 (2014) 141–146.
[18] F. Bakare, L. Schieren, B. Rouxel, L. Jiang, T. Langan, A. Kupke, M. Weiss, T. Dorin, The impact of L12 dispersoids and strain rate on the Portevin-Le-Chatelier effect and mechanical properties of Al–Mg alloys, Mater. Sci. Eng., A 811 (2021), 141040.
[19] C.H. Cho, H.W. Son, J.C. Lee, K.T. Son, J.W. Lee, S.K. Hyun, Effects of high Mg content and processing parameters on Portevin-Le Chatelier and negative strain rate sensitivity effects in Al–Mg alloys, Mater. Sci. Eng., A 779 (2020) 139–151.

[20] Y. Li, B. Lu, W. Yu, J. Fu, G. Xu, Z. Wang, Two-stage homogenization of Al-Zn-Mg-Cu-Zr alloy processed by twin-roll casting to improve $L1_2$ Al_3Zr precipitation, recrystallization resistance, and performance, J. Alloys Compd. 882 (2021), 160789.

[21] M. Ninomiya, R. Ohte, T. Uesugi, Y. Takigawa, K. Higashi, Al-8Mg alloy with high strength and high ductility by addition of a grain boundary strengthening element, Mater. Lett. 245 (2019) 218–221.

[22] T. Tański, P. Snopiński, K. Prusik, M. Sroka, The effects of room temperature ECAP and subsequent aging on the structure and properties of the Al-3%Mg aluminium alloy, Mater. Char. 133 (2017) 185–195.

[23] E.L. Huskins, B. Cao, K.T. Ramesh, Strengthening mechanisms in an Al-Mg alloy, Mater. Sci. Eng., A 527 (2010) 1292–1298.

[24] T. Mukai, K. Higashi, S. Tanimura, Influence of the magnesium concentration on the relationship between fracture mechanism and strain rate in high purity Al-Mg alloys, Mater. Sci. Eng., A 176 (1994) 181–189.

[25] M.F. Ashby, The deformation of plastically non-homogeneous materials, Philos. Mag. A 21 (1969) 399–424.

[26] R.E. Stoller, S.J. Zinkle, On the relationship between uniaxial yield strength and resolved shear stress in polycrystalline materials, J. Nucl. Mater. 283–287 (2000) 349–352.

[27] H.R. Last, R.K. Garrett, Mechanical behavior and properties of mechanically alloyed aluminum alloys, Metall. Mater. Trans. A 27 (1996) 737–745.

[28] X. Huang, N. Hansen, N. Tsuji, Hardening by annealing and softening by deformation in nanostructured metals, Science 312 (2006) 249–251.